


Femoral cartilage damage occurs at the zone of femoral head necrosis and can be accurately detected on traction MR arthrography of the hip in patients undergoing joint preserving hip surgery

F. Schmaranzer ^{1,2*}, T. D. Lerch^{1,2}, S. D. Steppacher¹, K. A. Siebenrock¹,
E. Schmaranzer³ and M. Tannast^{1,4}

¹Department of Orthopaedic Surgery, Inselspital Bern, University of Bern, Freiburgstrasse, 3010 Bern, Switzerland,

²Department of Diagnostic, Interventional and Pediatric Radiology, Inselspital Bern, University of Bern, Freiburgstrasse 3010 Bern, Switzerland,

³Department of Radiology, District Hospital St. Johann in Tirol, Freiburgstrasse, 6380 St. Johann in Tirol, Austria and

⁴Department of Orthopaedic Surgery and Traumatology, Fribourg Cantonal Hospital, University of Fribourg, Chemin des Pensionnats, 1752 Villars-sur-Glâne, Switzerland.

*Correspondence to: F. Schmaranzer. E-mail: florian.schmaranzer@insel.ch

Submitted 26 November 2020; revised version accepted 8 April 2021; accepted 12 April 2021

ABSTRACT

The primary purpose was to answer the following question: What is the location and pattern of necrosis and associated chondrolabral lesions and can they be accurately detected on traction MR arthrography compared with intra-operative findings in patients undergoing hip preservation surgery for femoral head necrosis (FHN)? Retrospective, diagnostic case series on 23 patients (23 hips; mean age 29 ± 6 years) with diagnosis of FHN undergoing open/arthroscopic joint preserving surgery for FHN and pre-operative traction MR arthrography of the hip. A MR-compatible device for weight-adapted application of leg traction (15–23 kg) was used and coronal, sagittal and radial images were acquired. Location and pattern of necrosis and chondrolabral lesions was assessed by two readers and compared with intra-operative findings to calculate diagnostic accuracy of traction MR arthrography. On MRI all 23 (100%) hips showed central FHN, most frequently antero-superiorly (22/23, 96%) where a high prevalence of femoral cartilage damage was detected (18/23, 78%), with delamination being the most common (16/23, 70%) damage pattern. Intra-operative inspection showed central femoral head cartilage damage most frequently located antero-superiorly (18/23, 78%) with femoral cartilage delamination being most common (14/23, 61%). Traction MR arthrography enabled detection of femoral cartilage damage with a sensitivity/specificity of 95%/75% for reader 1 and 89%/75% for reader 2. To conclude, femoral cartilage damage occurs at the zone of necrosis and can be accurately detected using traction MR arthrography of the hip which may be helpful for surgical decision making in young patients with FHN.

INTRODUCTION

Femoral head necrosis (FHN) is a major cause of osteoarthritis of the hip joint [1]. In young patients, efforts are made to halt the course of osteoarthritis. Two distinct surgical principles have been applied traditionally to treat FHN. Core decompression [2, 3] and vascularized bone grafting [3, 4] aim to restore femoral head blood supply. Rotational [5, 6] or angular [7] femoral osteotomies

are performed to position healthy bone into the main weight-bearing areas to prevent collapse and allow healing of the necrotic area. Historically these procedures have been performed from an extra-articular approach. More recently, open [8–14] and arthroscopic [15–17] procedures for surgical treatment of FHN have been described which offer direct access to the joint for bone grafting and chondrolabral repair [18].

To date, the optimal surgical treatment for FHN remains controversial [1]. This may be related to the fact that surgical planning often relies on imaging studies which allow staging of the disease but do not provide further information on location and extent of intra-articular damage [19]. More specifically the use of standard imaging MRI planes does not enable an exact localization of necrosis [19]. In contrast radial images which are oriented perpendicular to the femoral neck could potentially allow an accurate anatomic allocation of FHN, comparable to imaging of the cam deformity [20]. Currently, a detailed pre-operative image analysis of intra-articular damage in FHN is lacking [19], despite its detrimental effect on outcome of joint preserving surgery for FHN [21]. Such information could be valuable for planning of chondrolabral repair surgery [18]. MRI of the hip, even after intra-articular contrast injection often fails to detect hip cartilage damage [22, 23]. Typically, the tight coaptation of the hip prevents contrast accumulation which makes differentiation of cartilage layers difficult [22]. Recently application of leg traction during MR arthrography of the hip was introduced to overcome this problem and has shown promising first results in detection of intra-articular lesions in FAI [24–26]. Therefore, it was hypothesized that traction MR arthrography with radial imaging could be useful in the pre-operative characterization of FHN and associated chondrolabral lesions.

The primary purpose was to answer the following question: What is the location and pattern of necrosis and associated chondrolabral lesions and can they be accurately detected on traction MR arthrography compared with intra-operative findings in patients undergoing hip preservation surgery for FHN?

MATERIALS AND METHODS

Patients

After IRB-approval a retrospective, diagnostic study on patients with FHN diagnosed was performed between January 2016 and June 2019 at a tertiary hip preservation centre. Pre-operative diagnosis of FHN was based on the presence of a geographical low signal band on MRI according to the revised Association Research Circulation Osseous (ARCO) [27]. The institutional database was searched for patients undergoing open or arthroscopic reconstructive hip surgery for treatment of FHN with complete intra-articular inspection. Out of 27 patients (27 hips), 23 patients (23 hips) had pre-operative traction MR arthrography of the hip according to the institutional routine protocol and were included in the study.

Mean age was 29 ± 6 years (11 men, 45%; Table 1). Most frequently FHN occurred idiopathic (14/23, 61%). The majority of hips (16/23; 70%) were diagnosed with advanced ARCO Stage III [27]. Nine hips (9/23, 39%) had Tönnis Grade 0, and 14 hips (14/23, 61%) had Tönnis Grade 1 of radiographic osteoarthritis [28] (Table 1).

Diagnostic imaging

All patients underwent standardized supine radiographic imaging of the pelvis including antero-posterior (AP) pelvis views and cross-table lateral views [29]. All patients underwent traction MR arthrography following fluoroscopy guided injection. Intra-articular needle position was confirmed with 1–2 ml of iodinated contrast agent (iopamidol, 200 mg/ml; Iopamiro 200; Bracco) and 15–20 ml of diluted MR contrast agent (gadoteric acid, 0.0025 mmol/ml; Guerbet) were injected. MRI was performed at 3T (Skyra, Siemens Medical Solutions) using a large flexible body coil. An MR-compatible traction device (trac-view, Menges Medical) was used which includes a pulley, a cable connected to the weight and a supporting plate for the contralateral foot to prevent tilting of the pelvis [30, 31]. Traction load was adjusted depending on patient's weight: for patients weighing <60/60–80/>80 kg were used 15/18/23 kg, respectively. Coronal and sagittal proton-density (PD) weighted turbo spin-echo images without fat-saturation were acquired: repetition time (TR)/echo time (TE), 2600/11 ms, slice thickness of 2 mm, 170×170 mm field of view, a matrix size of 269×384 , acquisition time (AT) of 3–4 min. Radial PD-weighted turbo spin-echo images without fat-saturation were oriented around the femoral neck axis [20, 32]: TR/TE, 2100/14 ms, slice thickness of 4 mm, 170×170 mm field of view, a matrix size of 403×448 , AT of 5 min for 12 slices.

Surgical treatment

Twenty-three patients (23 hips) underwent joint preserving surgery, which was performed by three experienced hip surgeons (Table 1). In six hips (6/23, 26%) hip arthroscopy was performed including core decompression. In 17 hips (17/23, 74%), surgical hip dislocation was performed with direct treatment of the necrotic lesion at the femoral head performed in 14 hips (14/23, 61%). Most commonly curettage of the necrotic bone was performed, followed by impaction bone grafting and suturing of the femoral head cartilage (7/23, 30%) (Fig. 1) or autologous matrix-assisted chondrogenesis (3/23, 13%) [10]. Labral refixation was performed in nine hips (9/23, 39%) and subchondral drilling of the acetabulum was performed in five hips

Table I. Demographic and radiographic characteristics

Patients (hips)	23 (23)
Age (years)	29 ± 6
Men (%)	11 (45)
Body mass index (kg/m ²)	25 ± 3
Tönnis grade of osteoarthritis, hips (%)	Grade 0: 9 (39) Grade 1: 14 (61)
LCE angle (°)	28 ± 9
Hip dysplasia (LCE < 25°), hips (%)	7 (30)
Deep hip (LCE > 39°), hips (%)	1 (4)
Retroversion (positive COS, PWS and ISS signs), hips (%)	3 (12)
Alpha angle (°)	74 ± 12
Cam deformity ($\alpha > 60^\circ$), hips (%)	21 (91)
Aetiology, hips (%)	14 (61) idiopathic 6 (26) systemic/toxic 3 (13) post-traumatic
2019 revised ARCO criteria (0–IV), hips (%)	I (normal X-ray, MRI abnormal): 2 (9) II (X-ray abnormal, MRI abnormal): 5 (22) IIIA (subchondral fracture, depression ≤ 2 mm): 8 (35) IIIB (subchondral fracture, depression > 2 mm): 8 (35)
Previous surgery, hips (%)	2 (9) core decompression
Surgical approaches, hips (%)	8 (35) surgical hip dislocation 6 (26) surgical hip dislocation, femoral osteotomy 6 (26) hip arthroscopy, core decompression 3 (13) surgical hip dislocation, periacetabular osteotomy
Femoral osteochondroplasty, hips (%)	21 (91)
Chondrolabral repair, hips (%)	7 (30) curettage of necrosis, bone grafting and cartilage suture 3 (13) curettage of necrosis, bone grafting, AMIC 3 (13) subchondral drilling femoral head 1 (4) curettage of necrosis and osteochondral autograft 5 (22) subchondral drilling acetabulum 9 (39) labrum refixation

Values are expressed as mean ± SD with range in parentheses. COS, cross-over sign; PWS, posterior-wall sign; ISS, ischial-spine sign; AMIC, autologous matrix-assisted chondrogenesis; ARCO, association research circulation osseous; LCE, lateral center edge angle.

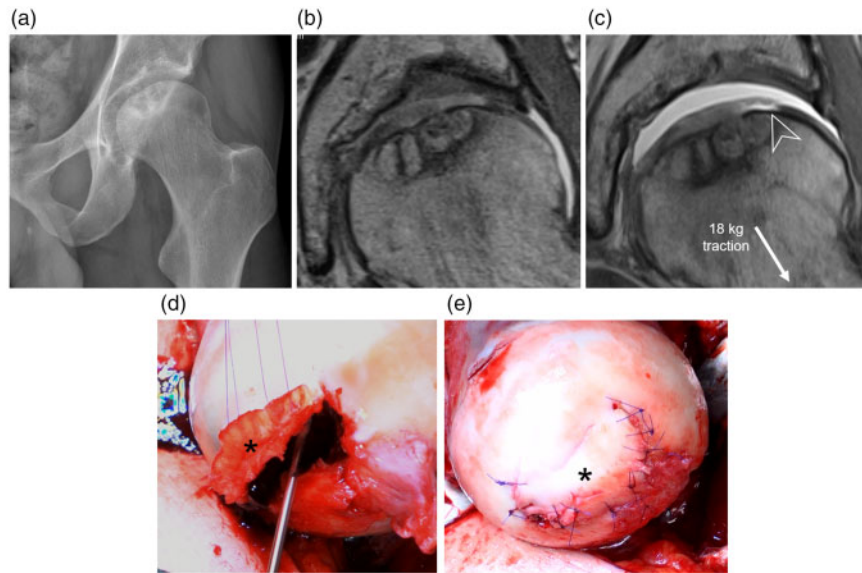


Fig. 1. (A) AP pelvis radiograph of a 43-year-old man with FHN ARCO Stage IIIB who underwent a ‘trapdoor procedure’ for osteochondral repair via a surgical hip dislocation. (B) Coronal PD-w MR arthrogram which was performed in an external institution shows no obvious femoral cartilage lesion. (C) MR arthrography was repeated with traction. Joint distraction was achieved, contrast agent entered the central compartment of the hip and a large centrally located cartilage flap became visible (arrowhead). (D) Extensive femoral cartilage delamination was confirmed at surgery. The cartilage flap was held aside (asterisk), to perform a curettage of the necrotic bone until bleeding was observed. The defect was filled with an autologous bone graft. (E) Final result after re-suturing of the cartilage flap (asterisk).

(5/23, 22%). Weight-bearing of the necrotic area was reduced with a concomitant femoral osteotomy in four hips [10]: three hips (3/23, 13%) inter-trochanteric varus-derotation osteotomies, one hip (1/23, 4%) posterior rotational femoral neck osteotomy. In two hips (8%), subtrochanteric derotation osteotomies were performed for correction of excessively high femoral version [33, 34]. Femoral osteochondroplasty was performed in 21 hips (21/23, 91%). In all patients, presence, location and damage pattern of intra-articular lesions was recorded intra-operatively according to the grading of Beck *et al.* [35]. For comparison with imaging findings surgical records were reviewed by an orthopaedic surgeon and femoroacetabular cartilage was graded: intact/delamination/thinning/defect. The acetabular labrum was graded as intact/chondrolabral separation/complex tear.

Image analysis

Radiographs were assessed by one senior orthopaedic surgeon for staging of FHN according to the 2019 revised ARCO grading [27]. The lateral-centre edge angle was measured, presence of acetabular retroversion (cross-over sign, posterior-wall sign and ischial-spine sign) was assessed [36] and the Tönnis grade of osteoarthritis [28] was evaluated. MRI analysis was performed independently from each other, blinded

to the initial report and the surgical report by a radiology resident and a senior radiologist (7 and 19 years of experience).

Radial images were used to assess the location of FHN at each half-hour position of the clock-face. Image criterion for FHN was defined as the presence of a geographical, hypointense line in the femoral head and was recorded dichotomously (yes/no) [19]. On each radial image a line perpendicular to the femoral neck axis was drawn for definition of central (medial to the perpendicular line) or peripheral (lateral to the perpendicular line) FHN (Fig. 2). Anatomic allocation of FHN was performed using a previously described approach (see below) [20].

Coronal-, sagittal- and radial- traction MR images were used to assess chondrolabral lesions. Definite anatomic allocation of lesions to the corresponding clock-face positions was performed on the 12 radial images using a previously validated technique [20, 32]: Each image represents a ‘half-hour’ position and can be allocated according anatomic landmarks. For necrosis and femoral cartilage damage the greater trochanter served as landmark for the femoral 12 o’clock position. For acetabular cartilage and labrum lesions the acetabular teardrop served as landmark for the acetabular 6 o’clock position. Accordingly, the acetabulum and femur were divided into four quadrants: 12–2:30 o’clock = antero-superior; 3–5:30 o’clock = antero-

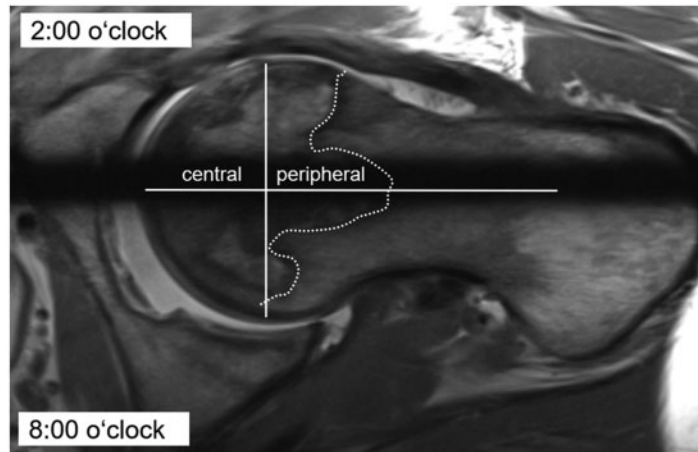


Fig. 2. Differentiation between peripheral and central location of FHN and femoral cartilage damage is shown on a radial image. This is based on a line which is drawn perpendicular to the femoral neck axis. If the lesion is medial/lateral to this line it is referred to as being located central/peripheral, respectively. In this hip peripheral and central FHN (dashed line) was present at the 2 o'clock and at the 8 o'clock position.

inferior; 6–8:30 o'clock = postero-inferior and 9–11:30 o'clock = postero-superior.

Femoral and acetabular cartilage lesions were graded using previously described classifications: delamination (subchondral contrast accumulation), thinning (partial-thickness loss of cartilage), defect (full-thickness loss of cartilage; Fig. 3) [24, 37]. Femoral cartilage lesions were further divided into peripheral and centrally located lesions. Labrum lesions were graded as chondrolabral separation (contrast extending into the labral base) or complex tear (contrast extension into the labral base and within the labral substance) [24, 37].

Statistical analysis

Descriptive statistics including mean and SD were calculated. Inter-observer reproducibility and intra-observer reliability were assessed using Cohen's kappa: < 0 poor agreement; 0.0–0.2, slight agreement; 0.21–0.4 fair agreement; 0.41–0.6, moderate agreement; 0.61–0.8, substantial agreement; 0.81–1, almost perfect agreement [38]. Sensitivity, specificity, accuracy, positive predictive value and negative predictive value of traction MR arthrography for detecting intra-articular lesions was calculated. SPSS version 25.0 (IBM, Armonk, New York, USA) was used for statistical analysis.

RESULTS

On MRI all 23 (100%) hips showed central FHN, which was most frequently located in the antero-superior (22/23, 96%) quadrant. Peripheral FHN was present in 8/23

(35%) hips, most frequently located in the antero-superior and -inferior quadrants (each 3/34, 13%; Fig. 4).

On traction MR arthrography most hips (19/23, 83%) demonstrated central femoral cartilage damage, most frequently located antero-superiorly (18/23, 78%). Femoral cartilage delamination was the most commonly (16/23, 70%) observed damage pattern (Fig. 4). Corresponding to that, intra-operative inspection showed central femoral head cartilage damage in the majority of the hips (19/23, 83%) most frequently located antero-superiorly (18/23, 78%), with femoral cartilage delamination being most common (14/23, 61%; Fig. 4). Traction MR arthrography enabled detection of femoral cartilage damage with a sensitivity/specificity of 95%/75% for Reader 1 and 89%/75% for Reader 2 (Table II; Figs 1 and 5). MRI grading of femoral cartilage lesions was consistent with surgical grading in 70% (16/23) of the cases for reader 1 ($\kappa = 0.427$, $P = 0.002$) and in 61% (14/23) of the cases for reader 2 ($\kappa = 0.403$, $P = 0.001$; Table III).

On MRI and at surgical inspection acetabular cartilage damage was present in 83% (19/23) and 87% (20/23) of the hips and was located most frequently antero-superiorly for both MRI (83%, 19/23) and at surgery (87%, 20/23), respectively (Fig. 6). Among the observed lesions acetabular cartilage delamination was most commonly observed on MRI (13/23, 57%) and intra-operatively (11/23, 48%; Fig. 6). Traction MR arthrography enabled detection of acetabular cartilage damage with a sensitivity/specificity of 90%/67% for reader 1 and 95%/33% for Reader 2 (Tables II and III). On MRI and at surgical inspection labrum lesions were present in 87% (20/23) of hips and

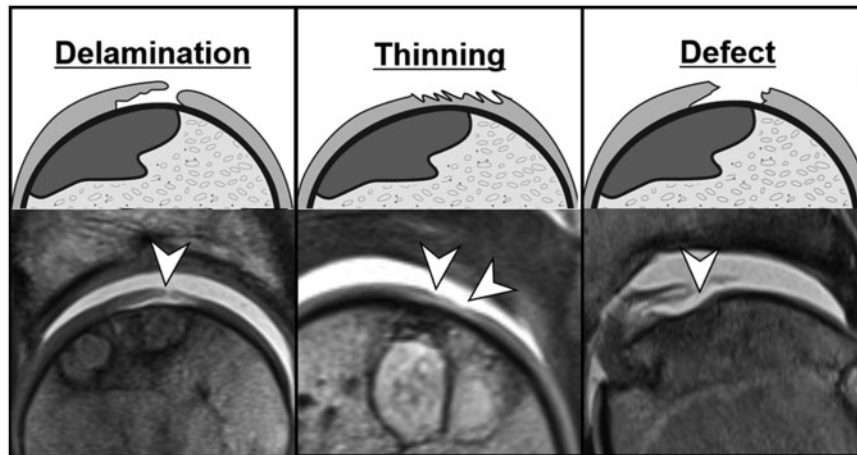


Fig. 3. Schematic drawings of femoral cartilage damage and corresponding appearance of femoral cartilage lesions on traction MR arthrography. (A) Delamination: subchondral contrast accumulation (arrowhead). (B) Thinning: partial-thickness loss of cartilage (arrowheads). (C) Defect: full-thickness loss of cartilage (arrowhead).

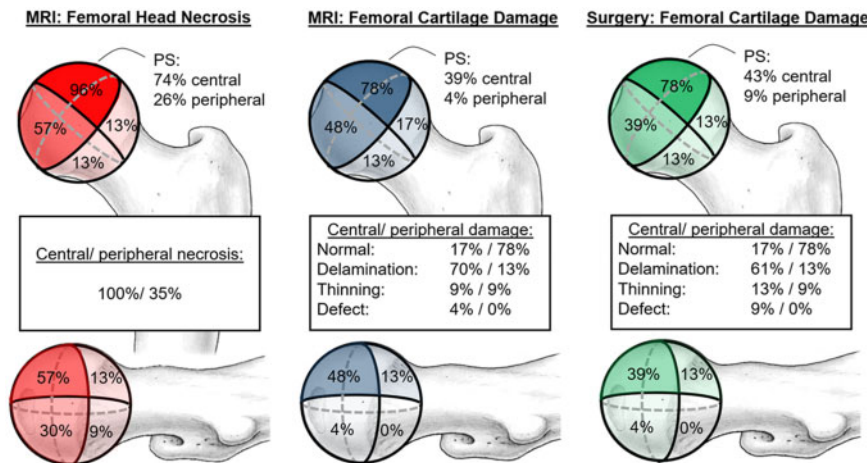


Fig. 4. Location of necrosis (left image), femoral cartilage damage assessed on MRI (middle image) and intra-operatively (right image) are shown from an antero-posterior (images on top) and lateral perspective (images at bottom). PS indicates the postero-superior quadrant. Necrosis was most commonly (96%) located at central antero-superior femoral head, the location where femoral cartilage damage was most commonly observed on MRI and intra-operatively (each 78%). Among the observed lesions femoral cartilage delamination was the most common damage pattern on MRI (70%) and at surgical inspection (61%).

91% (21/23) of hips, with 87% (20/23) and 91% (21/23) being located antero-superiorly, respectively. Most commonly the lesions were consistent with labro-chondral separation (MRI: 10/23, 43%; surgery: 13/23, 57%; Fig. 7). Traction MR arthrography enabled detection of labrum damage with a sensitivity/specificity of 95%/100% for Reader 1 and 100%/100% for Reader 2 (Tables II and III).

Substantial agreement ($\kappa = 0.747$, $P < 0.001$) between the two observers was observed for detection of FHN. Inter-observer agreement was moderate for grading of femoral- ($\kappa = 0.588$, $P < 0.001$) and acetabular cartilage

lesions ($\kappa = 0.417$, $P < 0.001$), and substantial for grading of labrum lesions ($\kappa = 0.633$, $P < 0.001$; Table II).

DISCUSSION

Although FHN is a well-known pre-arthritis condition and many surgical treatment concepts have been proposed, a concise pre-operative description of location and pattern of necrosis and associated chondrolabral damage is currently lacking [1]. It could be shown that damage to femoral head cartilage is located at the zone of FHN most commonly affecting the central part of the antero-superior

Table II. Diagnostic performance of traction MR arthrography in detection of chondrolabral lesions compared with surgery

Parameter	Femoral cartilage		Acetabular cartilage		Labrum	
	Reader 1	Reader 2	Reader 1	Reader 2	Reader 1	Reader 2
No. of true-positives, (no. of hips)	18	17	18	19	20	21
No. of false-negatives, (no of hips)	1	2	2	1	1	0
No. of true-negatives, (no. of hips)	3	3	2	1	2	2
No. of false-positives (no. of hips)	1	1	1	2	0	0
Sensitivity (%)	95 (74–100)	89 (67–99)	90 (68–99)	95 (75–100)	95 (76–100)	100 (84–100)
Specificity (%)	75 (19–99)	75 (19–99)	67 (9–99)	33 (1–91)	100 (16–100)	100 (16–100)
Positive predictive value (%)	95 (77–99)	94 (76–99)	95 (78–99)	90 (81–96)	100 (100–100)	100 (100–100)
Negative predictive value (%)	75 (29–96)	60 (26–86)	50 (18–82)	50 (8–92)	67 (23–93)	100 (100–100)
Accuracy (%)	91 (72–99)	87 (66–97)	87 (66–97)	87 (66–97)	96 (78–100)	100 (85–100)
Inter-observer agree- ment (Cohen's κ)*	0.588		0.417		0.633	

Numbers in parentheses are 95% CIs.

*P values \leq 0.001.

femoral head. Traction MR arthrography was highly accurate in detecting chondrolabral lesions and allowed grading of chondrolabral lesions with moderate to substantial agreement between imaging and surgical findings.

Despite the fact that location of necrosis affects outcome of core decompression, femoral osteotomies and vascularized fibular grafting for treatment of FHN a detailed analysis of location of FHN is currently lacking [1]. Location of necrosis has been commonly described on coronal and sagittal MR images [39]. However due to their orientation, imaging planes which are not oriented perpendicular to the femoral neck preclude an accurate anatomic allocation [37]. Recently, the use of radial MRI has been proposed for planning the correction angle in rotational femoral osteotomy based on the location and extent of FHN relative to the remaining healthy bone [40]. By using radial MRI, a detailed topographical description of necrosis could be provided with good inter-observer agreement between two readers and identified the central antero-superior (96% of hips) quadrant as predominant location of

FHN (Fig. 4). Since radial imaging is widely used as gold-standard for visualization of the cam deformity, implementation of radial images into a routine MR protocol for FHN may be straightforward [41].

Subcortical fractures and femoral head collapse are pathognomonic signs of advanced FHN [39]. However, there is limited data regarding the associated damage to the overlying femoral head cartilage. Despite advances in modern MR techniques such as high-field scanners, improved coil design and high-resolution sequences, imaging of cartilage lesions remains challenging in the hip [42]. In the first study, comparing non-contrast MRI with arthroscopic detection of joint damage in FHN, Ruch *et al.* [43] showed that MRI cannot reliably detect femoral cartilage damage. The authors recommended diagnostic hip arthroscopy in FHN to decide between vascularized fibular grafting or total hip replacement based on the already present arthritic changes [43]. Using current state of the art MRI at 3T Shoji *et al.* [21] reported that non-contrast MRI of the hip could detect articular cartilage damage in

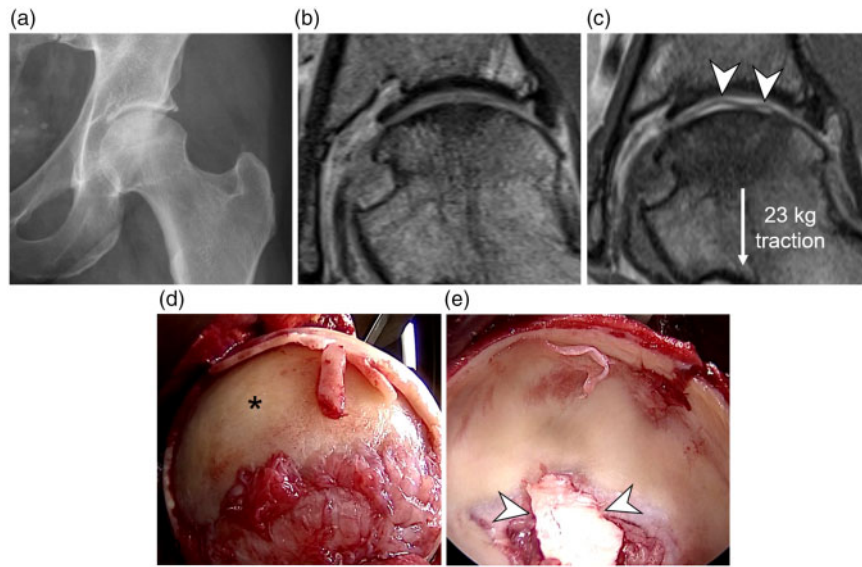


Fig. 5. AP pelvis radiograph of a 36-year-old woman with FHN ARCO Stage IIIA undergoing a surgical hip dislocation and autologous matrix-induced chondrogenesis. (B) Coronal PD-w MR arthrogram which was performed in an external institution shows no obvious femoral cartilage lesion. (C) Two months later MR arthrography was repeated with leg traction. Minimal joint distraction was achieved but extensive subchondral contrast accumulation (arrowheads) became visible indicating femoral cartilage delamination involving two thirds of the weight-bearing surface. (D, E) Delaminated femoral cartilage got completely detached during the dislocation manoeuvre and was found lying in the acetabulum (arrowheads) leaving a large cartilage femoral cartilage defect (asterisk).

only 32% of the cases compared with arthroscopic staging of joint damage when a femoral osteotomy was planned. To improve the otherwise poor visualization of the femoral head cartilage in FHN, application of traction during MRI of the hip has been first described more than 20 years ago using non-contrast MRI combined with 10–15 kg of traction in five patients undergoing hip arthroplasty [44].

A modified traction technique for MR arthrography was used in this study which is similar to the arthroscopic approach to gain access to the central joint compartment. This includes intra-articular contrast injection to break the suction seal, a weight-adapted traction force and a supporting plate for the contralateral leg to stabilize the pelvis [30, 45]. In contrast to previous reports this enabled us to detect femoral and acetabular cartilage damage in FHN with high sensitivity ranging from 89–95% to 90–95%, respectively (Figs 1 and 5). Thus, instead of performing surgery for diagnostic purposes cartilage damage may be assessed with traction MR arthrography to identify those patients who may still benefit from joint preserving surgery for FHN or should be rather considered for hip replacement thereby reducing costs and number of subsequent surgeries. Additionally, a more detailed assessment of pre-operative cartilage damage may be helpful to determine cases in which a femoral cartilage repair may be beneficial. This is important as femoral cartilage repair usually requires an open surgical approach to the hip.

Using MRI with intra-operative comparison femoral cartilage delamination was the predominant pattern of damage to the central, antero-superior femoral head where FHN was most frequently detected (Figs 1, 2 and 5). This supports the concept of cartilage debonding occurring secondary to underlying subchondral fractures [43, 44]. The imaging findings observed in this study may have potential implications for planning of femoral cartilage repair surgery in FHN for which promising short-term outcome have been reported even in cases with large necrotic lesions [10, 11, 13]. Delaminated but otherwise intact femoral cartilage may be treated with curettage of necrosis, bone grafting and re-suturing of the cartilage flap (so called ‘trapdoor procedure’; Fig. 1) [10, 12], full-thickness defects may be treated with osteochondral grafts [13] or autologous matrix-induced chondrogenesis (Fig. 5) [11].

Furthermore, we could confirm findings of previous studies reporting a high prevalence of acetabular cartilage- and labrum lesions [8, 43, 46]. Interestingly, these lesions were predominantly present in the antero-superior quadrant and most frequently acetabular cartilage delamination and chondrolabral separation were observed (Figs 6 and 7). This location and damage pattern resemble the characteristic findings of cam-type FAI [35]. Thus, it has been suggested that these lesions are caused by an inclusion, cam-type mechanism subsequent to flattening of the femoral neck-junction in FHN [8]. Indeed, the majority of

Table III. Grading of chondrolabral lesions: traction MR arthrography versus hip surgery

MRI: femoral cartilage (Reader 1/2)	Surgery: femoral cartilage				Total
	Intact	Delamination	Thinning	Defect	
Intact	3/3	1/2	0/0	0/0	4/5
Delamination	0/0	13/9	2/0	1/1	16/10
Thinning	1/1	0/2	0/2	1/1	2/6
Defect	0/0	0/1	1/1	0/0	1/2
Total	4	14	3	2	23

Concordant grading*—Reader 1: 16 (70%) $\kappa = 0.427$ and Reader 2: 14 (61%) $\kappa = 0.403$

MRI: acetabular cartilage (reader 1/2)

	Surgery: acetabular cartilage				Total
	Intact	Delamination	Thinning	Defect	
Intact	2/1	1/1	1/0	0/0	4/2
Delamination	1/1	9/8	2/0	1/1	13/10
Thinning	0/1	0/0	3/6	1/0	4/7
Defect	0/0	1/2	0/0	1/2	2/4
Total	3	11	6	3	23

Concordant grading*—Reader 1: 15 (65%) $\kappa = 0.465$ and Reader 2: 17 (74%) $\kappa = 0.616$

MRI: labrum (reader 1/2)	Surgery: labrum			Total
	Intact	Chondrolabral separation	Complex tear	
Intact	2/2	1/0	0/0	3/2
Chondrolabral separation	0/0	9/8	1/2	10/10
Complex tear	0/0	3/5	7/6	10/11
Total	2	13	8	23

Concordant grading*—Reader 1: 18 (78%) $\kappa = 0.633$ and Reader 2: 16 (70%) $\kappa = 0.476$

*P values ≤ 0.002 .

patients presented with a cam deformity and a concomitant femoral osteochondroplasty was performed in 91% of the cases in this study. However, based on this observation alone it is not possible to draw any definite conclusions and further studies are needed to determine the aetiology of cam deformities and their significance in patients with FHN.

This study has a number of limitations. First, a relatively small group of patients with FHN was included which reflects the rare nature of the disease in young patients. However, according to the performed literature review this study includes the largest group of patients with FHN undergoing joint preserving surgery including comparison with pre-operative traction MR arthrography of the hip.

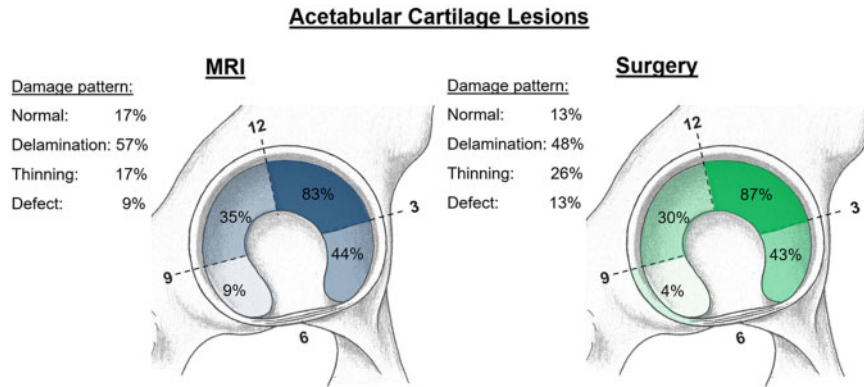


Fig. 6. Location and pattern of acetabular cartilage lesions on MRI (left image) and at intra-operative inspection (right image). On both MRI and at surgical inspection the antero-superior quadrant was most frequently affected (83% and 87%) and cartilage delamination was most common (57% and 48%).

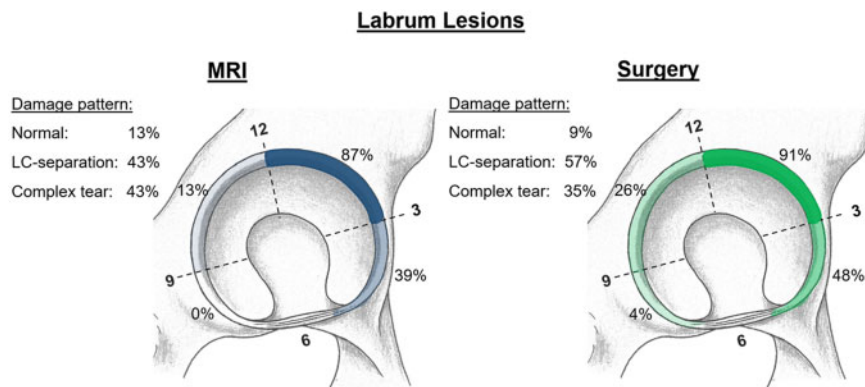


Fig. 7. Location and pattern of labrum damage on MRI (left image) and at intra-operative inspection (right image). On both MRI and at surgical inspection the antero-superior quadrant was most frequently affected (87% and 91%) and chondrolabral separation was most common (43% and 57%).

Second, the imaging protocol did not allow a direct comparison with standard MR arthrography obtained without traction as this was not feasible in a busy clinical setup. Future studies are needed to assess whether there is a benefit in diagnostic accuracy when applying traction to the hip during MRI compared with standard MRI techniques. Third, no clinical follow-up is presented since this was beyond the scope of this study. Thus, no comments regarding the surgical outcome and the predictive value of these imaging findings can be made.

To conclude, femoral cartilage damage occurs at the zone of FHN and can be accurately detected using traction MR arthrography of the hip. Based on these findings, pre-operative traction MR arthrography may have potential to better inform surgeons as they contemplate whether to perform total hip arthroplasty or joint preserving treatment with/without osteochondral repair in young patients with FHN.

FUNDING

One of the authors (F.S.) received funding from the Clinical Trials Unit of the University of Bern during the conduction of this study. The remaining authors certify that neither he, nor any member of his immediate family, has funding or commercial associations (consultancies, stock ownership, equity interest, patent/licensing arrangements etc.) that might pose a conflict of interest in connection with the submitted article.

CONFLICT OF INTEREST STATEMENT

None declared.

REFERENCES

1. Chughtai M, Piuizzi NS, Khlopas A *et al.* An evidence-based guide to the treatment of osteonecrosis of the femoral head. *Bone Joint J* 2017; **99-B**: 1267–79.
2. Camp JF, Colwell CW. Core decompression of the femoral head for osteonecrosis. *J Bone Joint Surg Am* 1986; **68**: 1313–9.

3. Cao L, Guo C, Chen J *et al.* Free vascularized fibular grafting improves vascularity compared with core decompression in femoral head osteonecrosis: a randomized clinical trial. *Clin Orthop Relat Res* 2017; **475**: 2230–40.
4. Judet H, Judet J, Gilbert A *et al.* Treatment of idiopathic necrosis of the femoral head by a vascularized fibular graft. Evaluation after 7 years' experience. *Chirurgie* 1986; **112**: 699–702.
5. Sugioka Y, Katsuki I, Hotokebuchi T. Transtrochanteric rotational osteotomy of the femoral head for the treatment of osteonecrosis. Follow-up statistics. *Clin Orthop Relat Res* 1982; **169**: 115–26.
6. Ishikwa T, Atsumi T, Tamaoki S *et al.* Early repair of necrotic lesion of the femoral head after high-degree posterior rotational osteotomy in young patients—a study evaluated by volume measurement using magnetic resonance imaging. *J Hip Preserv Surg* 2015; **2**: 145–51.
7. Zhao G, Yamamoto T, Ikemura S *et al.* Radiological outcome analysis of transtrochanteric curved varus osteotomy for osteonecrosis of the femoral head at a mean follow-up of 12.4 years. *J Bone Joint Surg Br* 2010; **92-B**: 781–6.
8. Kloen P, Leunig M, Ganz R. Early lesions of the labrum and acetabular cartilage in osteonecrosis of the femoral head. *J Bone Joint Surg Br* 2002; **84**: 66–9.
9. Cheng Q, Zhao F-C, Xu S-Z *et al.* Modified trapdoor procedures using autogenous tricortical iliac graft without preserving the broken cartilage for treatment of osteonecrosis of the femoral head: a prospective cohort study with historical controls. *J Orthop Surg* 2020; **15**: 183.
10. Steppacher SD, Sedlmayer R, Tannast M *et al.* Surgical hip dislocation with femoral osteotomy and bone grafting prevents head collapse in hips with advanced necrosis. *Hip Int J Clin Exp Res Hip Pathol Ther* 2020; **30**: 398–406.
11. Leunig M, Tibor LM, Naal FD *et al.* Surgical technique: second-generation bone marrow stimulation via surgical dislocation to treat hip cartilage lesions. *Clin Orthop Relat Res* 2012; **470**: 3421–31.
12. Mont MA, Einhorn TA, Sponseller PD *et al.* The trapdoor procedure using autogenous cortical and cancellous bone grafts for osteonecrosis of the femoral head. *J Bone Joint Surg Br* 1998; **80**: 56–62.
13. Johnson JD, Desy NM, Sierra RJ. Ipsilateral femoral head osteochondral transfers for osteochondral defects of the femoral head. *J Hip Preserv Surg* 2017; **4**: 231–9.
14. Leibold CS, Schmaranzer F, Siebenrock K-A *et al.* Femoral osteotomies for the treatment of avascular necrosis of the femoral head. *Oper Orthopadie Traumatol* 2020; **2**: 116–126
15. Beck DM, Park BK, Youm T *et al.* Arthroscopic treatment of labral tears and concurrent avascular necrosis of the femoral head in young adults. *Arthrosc Tech* 2013; **2**: e367–71.
16. Nazal MR, Parsa A, Martin SD. Mid-term outcomes of arthroscopic-assisted Core decompression of Precollapse osteonecrosis of femoral head—minimum of 5 year follow-up. *BMC Musculoskelet Disord* 2019; **20**: 448.
17. Gupta AK, Frank RM, Harris JD *et al.* Arthroscopic-assisted core decompression for osteonecrosis of the femoral head. *Arthrosc Tech* 2014; **3**: e7–11.
18. Papavasiliou A, Yercan HS, Koukoulis N. The role of hip arthroscopy in the management of osteonecrosis. *J Hip Preserv Surg* 2014; **1**: 56–61.
19. Karantanas AH, Drakonaki EE. The role of MR imaging in avascular necrosis of the femoral head. *Semin Musculoskelet Radiol* 2011; **15**: 281–300.
20. Klenke FM, Hoffmann DB, Cross BJ *et al.* Validation of a standardized mapping system of the hip joint for radial MRA sequencing. *Skeletal Radiol* 2015; **44**: 339–43.
21. Shoji T, Yamasaki T, Ota Y *et al.* Intra-articular pathology affects outcomes after joint preserving surgery for osteonecrosis of the femoral head. *Int Orthop* 2020; **44**: 1295–1303.
22. Pfirrmann CWA, Duc SR, Zanetti M *et al.* MR arthrography of acetabular cartilage delamination in femoroacetabular cam impingement. *Radiology* 2008; **249**: 236–41.
23. Schmaranzer F, Kheterpal AB, Bredella MA. Best practices: hip femoroacetabular impingement. *AJR Am J Roentgenol* 2021; **216**: 585–98.
24. Schmaranzer F, Klauser A, Kogler M *et al.* Diagnostic performance of direct traction MR arthrography of the hip: detection of chondral and labral lesions with arthroscopic comparison. *Eur Radiol* 2015; **25**: 1721–30.
25. Schmaranzer F, Klauser A, Kogler M *et al.* MR arthrography of the hip with and without leg traction: assessing the diagnostic performance in detection of ligamentum teres lesions with arthroscopic correlation. *Eur J Radiol* 2016; **85**: 489–97.
26. Schmaranzer F, Lerch TD, Strasser U *et al.* Usefulness of MR arthrography of the hip with and without leg traction in detection of intra-articular bodies. *Acad Radiol* 2019; **26**: e252–9.
27. Yoon B-H, Mont MA, Koo K-H *et al.* The 2019 Revised Version of Association Research Circulation Osseous Staging System of Osteonecrosis of the Femoral Head. *J Arthroplasty* 2020; **35**: 933–40.
28. Tönnis D. General radiography of the hip joint. In: Tönnis D (ed.). *Congenital Dysplasia, Dislocation of the Hip*. New York: Springer, 1987.
29. Tannast M, Siebenrock KA, Anderson SE. Femoroacetabular impingement: radiographic diagnosis—what the radiologist should know. *AJR Am J Roentgenol* 2007; **188**: 1540–52.
30. Schmaranzer F, Klauser A, Kogler M *et al.* Improving visualization of the central compartment of the hip with direct MR arthrography under axial leg traction: a feasibility study. *Acad Radiol* 2014; **21**: 1240–7.
31. Schmaranzer F, Cerezal L, Llopis E. Conventional and arthrographic magnetic resonance techniques for hip evaluation: what the radiologist should know. *Semin Musculoskelet Radiol* 2019; **23**: 227–51.
32. Schmaranzer F, Haefeli P, Hanke M *et al.* How does the dGEMRIC index change after surgical treatment for FAI? A prospective controlled study: preliminary results. *Clin Orthop Relat Res* 2017; **475**: 1080–99.
33. Lerch TD, Schmaranzer F, Steppacher SD *et al.* Most of patients with femoral derotation osteotomy for posterior extraarticular hip impingement and high femoral version would do surgery again. *Hip Int J Clin Exp Res Hip Pathol Ther* 2020; **1120700020953100** online ahead of print.
34. Schmaranzer F, Kallini JR, Miller PE *et al.* The effect of modality and landmark selection on MRI and CT femoral torsion angles. *Radiology* 2020; **296**: 381–90.
35. Beck M, Kalhor M, Leunig M *et al.* Hip morphology influences the pattern of damage to the acetabular cartilage:

- femoroacetabular impingement as a cause of early osteoarthritis of the hip. *J Bone Joint Surg Br* 2005; **87-B**: 1012–8.
36. Tannast M, Hanke MS, Zheng G *et al*. What are the radiographic reference values for acetabular under- and overcoverage? *Clin Orthop Relat Res* 2015; **473**: 1234–46.
 37. Schmaranzer F, Todorski IAS, Lerch TD *et al*. Intra-articular lesions: imaging and surgical correlation. *Semin Musculoskelet Radiol* 2017; **21**: 487–506.
 38. Landis JR, Koch GG. An application of hierarchical kappa-type statistics in the assessment of majority agreement among multiple observers. *Biometrics* 1977; **33**: 363–74.
 39. Gardeniers JWM, Gosling-Gardeniers AC, Rijnen WHC. The ARCO staging system: generation and evolution since 1991. In: Koo K-H, Mont MA, Jones LC (eds.). *Osteonecrosis*. Berlin, Heidelberg: Springer Berlin Heidelberg, 2014, 215–8.
 40. Atsumi T. Posterior rotational osteotomy for severe femoral head osteonecrosis. In: Koo K-H, Mont MA, Jones LC (eds.). *Osteonecrosis*. Berlin, Heidelberg: Springer Berlin Heidelberg, 2014, 331–7.
 41. Mascarenhas VV, Castro MO, Rego PA *et al*. The lisbon agreement on femoroacetabular impingement imaging-part 1: overview. *Eur Radiol* 2020; **30**: 6966–7.
 42. Albers CE, Wambeek N, Hanke MS *et al*. Imaging of femoroacetabular impingement-current concepts. *J Hip Preserv Surg* 2016; **3**: 245–61.
 43. Ruch DS, Sekiya J, Dickson Schaefer W *et al*. The role of hip arthroscopy in the evaluation of avascular necrosis. *Orthopedics* 2001; **24**: 339–43.
 44. Nakanishi K, Tanaka H, Nishii T *et al*. MR evaluation of the articular cartilage of the femoral head during traction. Correlation with resected femoral head. *Acta Radiol* 1999; **40**: 60–3.
 45. Byrd JW, Chern KY. Traction versus distension for distraction of the joint during hip arthroscopy. *Arthrosc J Arthrosc Relat Surg* 1997; **13**: 346–9.
 46. McCarthy J, Puri L, Barsoum W *et al*. Articular cartilage changes in avascular necrosis: an arthroscopic evaluation. *Clin Orthop Relat Res* 2003; **406**: 64–70.